NASA/TM—2000–210331

Loads Combination Research at Marshall Space Flight Center

R. Ferebee
Marshall Space Flight Center, Marshall Space Flight Center, Alabama

June 2000

The NASA STI Program Office...in Profile

Since its founding, NASA has been dedicated to the advancement of aeronautics and space science. The NASA Scientific and Technical Information (STI) Program Office plays a key part in helping NASA maintain this important role.

The NASA STI Program Office is operated by Langley Research Center, the lead center for NASA's scientific and technical information. The NASA STI Program Office provides access to the NASA STI Database, the largest collection of aeronautical and space science STI in the world. The Program Office is also NASA's institutional mechanism for disseminating the results of its research and development activities. These results are published by NASA in the NASA STI Report Series, which includes the following report types:

- TECHNICAL PUBLICATION. Reports of completed research or a major significant phase of research that present the results of NASA programs and include extensive data or theoretical analysis. Includes compilations of significant scientific and technical data and information deemed to be of continuing reference value. NASA's counterpart of peer-reviewed formal professional papers but has less stringent limitations on manuscript length and extent of graphic presentations.

- TECHNICAL MEMORANDUM. Scientific and technical findings that are preliminary or of specialized interest, e.g., quick release reports, working papers, and bibliographies that contain minimal annotation. Does not contain extensive analysis.

- CONTRACTOR REPORT. Scientific and technical findings by NASA-sponsored contractors and grantees.

- CONFERENCE PUBLICATION. Collected papers from scientific and technical conferences, symposia, seminars, or other meetings sponsored or cosponsored by NASA.

- SPECIAL PUBLICATION. Scientific, technical, or historical information from NASA programs, projects, and mission, often concerned with subjects having substantial public interest.

- TECHNICAL TRANSLATION. English-language translations of foreign scientific and technical material pertinent to NASA's mission.

Specialized services that complement the STI Program Office's diverse offerings include creating custom thesauri, building customized databases, organizing and publishing research results...even providing videos.

For more information about the NASA STI Program Office, see the following:

- Access the NASA STI Program Home Page at ***http://www.sti.nasa.gov***

- E-mail your question via the Internet to help@sti.nasa.gov

- Fax your question to the NASA Access Help Desk at (301) 621–0134

- Telephone the NASA Access Help Desk at (301) 621–0390

- Write to:
  NASA Access Help Desk
  NASA Center for AeroSpace Information
  7121 Standard Drive
  Hanover, MD 21076–1320

NASA/TM—2000–210331

Loads Combination Research at Marshall Space Flight Center

R. Ferebee
Marshall Space Flight Center, Marshall Space Flight Center, Alabama

National Aeronautics and
Space Administration

Marshall Space Flight Center • MSFC, Alabama 35812

June 2000

Available from:

NASA Center for AeroSpace Information
7121 Standard Drive
Hanover, MD 21076–1320
(301) 621–0390

National Technical Information Service
5285 Port Royal Road
Springfield, VA 22161
(703) 487–4650

TABLE OF CONTENTS

LIST OF FIGURES

LIST OF FIGURES (Continued)

LIST OF TABLES

LIST OF ACRONYMS

HF	high frequency
JSC	Johnson Space Center
LF	low frequency
MS	mean square
MSFC	Marshall Space Flight Center
OAST	Office of Aeronautics and Space Technology
PDF	probability distribution function
RMS	root mean square
RSS	root sum square
TC	time constant

TECHNICAL MEMORANDUM

LOAD COMBINATION RESEARCH AT MARSHALL SPACE FLIGHT CENTER

1. INTRODUCTION

The Marshall Space Flight Center (MSFC) loads combination research team was formed in 1983 under the direction of NASA Headquarters Office of Aeronautics and Space Technology (OAST). The purpose of the team was to investigate the methods of combining low-frequency transient loads with high-frequency random loads. Transient loads are produced by the Space Shuttle's response to transient events such as engine ignition, lift-off "twang," and staging, while random loads are induced by engine and aerodynamically generated noise impinging on the vehicle and payload structure, causing components to vibrate. There is considerable variation within the aerospace industry in the derivation and combination of these dynamic design loads. The loads combination team was charged with examining these techniques and determining a more realistic and consistent method of deriving and combining these loads. The team focused on four steps in the investigation:

1. Assess the applicability of Miles' relationship to establish random vibration design loads.

2. Investigate the time-consistent combination of transient and random loads. Support the findings with simple experiments.

3. Investigate phasing of the orthogonal axis loads versus worst-case single-axis loads.

4. Develop and implement a flight instrumentation package to support the loads combination rationale.

When the loads combination team was disbanded in 1989, step 1 had been completed and substantial progress had been made on step 2. The results of the Miles' relationship investigation were reported in reference 1 and presented at the Shuttle Payload Dynamic Environments and Loads Prediction Workshop held at the Jet Propulsion Laboratory in January 1984. What follows was written by the loads combination team (Jess Jones, Bob Walker, Robin Ferebee, and Ron Jewell from the MSFC Structural Dynamics Division) and specifically concentrates on a load combination pioneered by Dick Schock and Len Tuell and also reports on efforts to verify the different methods on Spacelab flight data.

2. LOADS COMBINATION

Design of components and structures consists of combining loads from two types of excitation. These are the low-frequency (0–50 Hz) and high-frequency (20–2,000 Hz) types of environmental loads.

Let $z(t)$ = the combined loads

$$z(t)=x(t)+y(t) \quad , \tag{1}$$

where:

$x(t)$ = low-frequency loads (transient)

$y(t)$ = high-frequency loads (random).

The problem becomes one of determining the statistics of $z(t)$ in terms of $x(t)$ and $y(t)$. Generally, the high-frequency load is in the form of random excitation with a Gaussian (normal) probability distribution. For the low-frequency environment, it is generally in the form of a decaying sine wave. For this analysis it is assumed that the combined loads can be described in this manner. For the sake of this investigation, assume $x(t)$ has the following form (shown in fig. 1).

$$\Psi(t)=Ae^{-\zeta\omega t}\sin(\omega t) \quad , \tag{2}$$

where:

$\zeta = C/C_c$ = damping/critical damping

$\omega = 2\pi f$ = natural frequency

$T=-\left(\frac{\pi}{2}\right)\frac{\ln(M)}{\zeta\omega}$ where M = ratio of amplitude at time T to maximum amplitude

A_0 = peak amplitude of decaying sine function; $A_0=\frac{A}{e^{\frac{\pi}{2}\left(\frac{\zeta}{\sqrt{1-\zeta^2}}\right)}}$.

The time constant of eq. (2) is normally defined as $1/(\zeta\omega)$; eq. (2) is, in effect, the impulse response or free decay response of a single degree-of-freedom system to unit impulse.

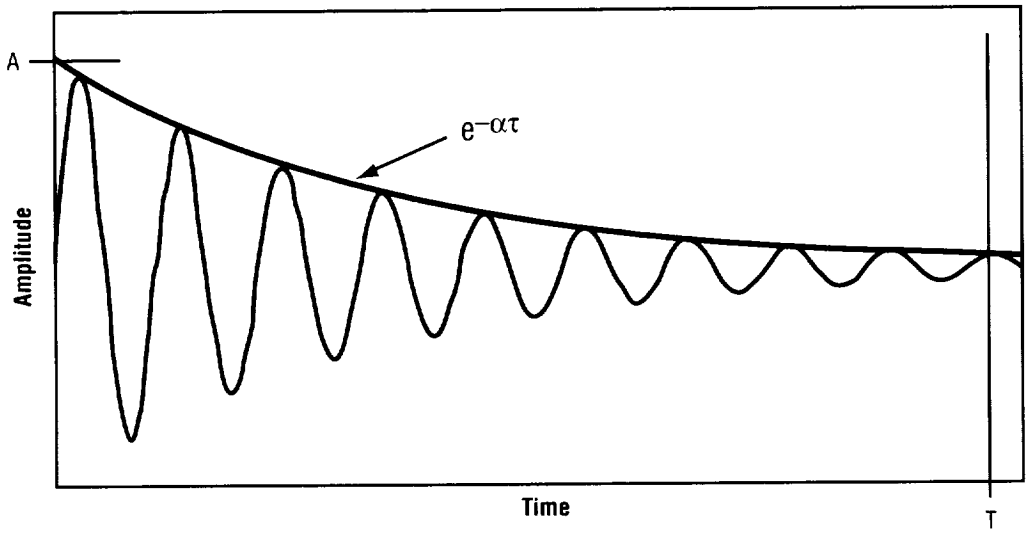

Figure 1. Damped sinusoid waveform.

Schock[2] presents a derivation of the probability density for a Gaussian noise signal combined with a damped sine wave of the form specified by eq. (1). His formulation has not been generalized, as his results are presented for $\omega = 1$. Therefore, following Schock, the probability density of a function as defined by eqs. (1) and (2) is

$$p(z) = \frac{1}{T}\sqrt{\frac{1}{2\pi\sigma_R{}^2}}\int_0^T e^{-\left(\frac{1}{2\sigma_R{}^2}\right)\left(z - Ae^{-\zeta\omega t}\sin(\omega t)\right)^2} dt \ . \tag{3}$$

where σ_R is the standard deviation of the random process; i.e., of $y(t)$, and T is taken to be the time interval required for the sine amplitude to decay to some prescribed level. This time is normally taken to be 4 or 5 time constants ($TC = 1/(\zeta\omega)$). In this analysis, $T = \ln(0.01)/\omega\zeta$ which allows the sine amplitude to decay to 1 percent of its peak value.

The distribution function of $z(t)$ is then

$$P(z) = \int_{-\infty}^{k} p(z)dz \ . \tag{4}$$

where k is set to the prescribed level (z) to achieve a certain probability level, for example 99.9 percent confidence.

In the case where damping is negligible, eq. (3) can be simplified to account for a sinusoid combined with random noise

$$p(z) = \frac{1}{T}\sqrt{\frac{1}{2\pi\sigma_R{}^2}}\int_0^T e^{-\left(\frac{1}{2\sigma_R{}^2}\right)\left(z - A\sin(\omega t)\right)^2} dt \ . \tag{5}$$

A plot of the probability distribution function (PDF) in eq. (1) for the case of σ_R=1 and A=10 shows the shape of the function for relatively low σ_R/A (fig. 2). The shape of the function rapidly approaches the familiar bell shape as σ_R/A approaches 1.

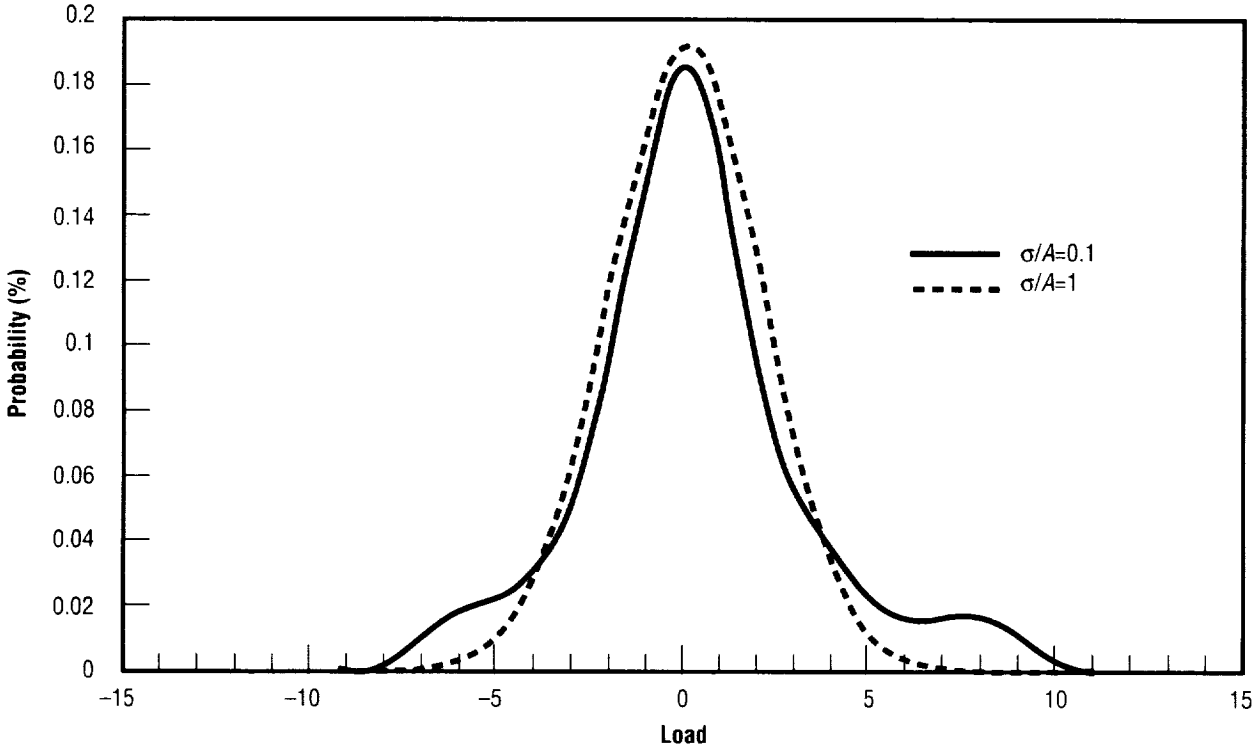

Figure 2. Plot of probability density function for damped sine and random combination.

Table 1 shows some examples of load combinations using conventional techniques and the method shown in the equations above. In the table, the 3σ and 2σ columns use eq. (4) with k chosen as 0.99865 and 0.975 respectively. The root sum square (RSS) Peaks column uses $\sqrt{A^2+(3\sigma)^2}$, Sum mean square (MS) is the sum of the MS values; $3\sqrt{\left(A/2\right)^2+\sigma^2}$, and Straight Sum is simply $A+3\sigma$. In all cases ω=1 and ζ=0.1. The last column is 3σ divided by the Straight Sum. The last row is a check on the accuracy of the method, which is within 1 percent of the actual values.

Table 1. Load combination for various ratios of random and damped sinusoids.

Random (σ) g_{rms}	Sine (A) g_{pk}	Random/ Sine	3σ	2σ	RSS Peaks	Sum MS	Straight Sum	Difference %
5	10	0.5	18.20	11.77	18.03	21.21	25.0	73
5	5	1	15.80	10.32	15.81	16.77	20.0	79
20	5	4	60.16	39.26	60.21	60.47	65.0	93
5	0	Large	14.98	9.75	15.00	15.00	15.0	100

As can be seen in the last column (Straight Sum divided by 3σ), the method shown herein reduces the magnitude of combined loads by varying amounts, depending on the Random/Sine ratio. By far the majority of cases are similar to the third row, with a relatively high random load. In this case the load is reduced by only 7 percent and is very close to the RSS method, which shows that the random loads (when squared) tend to drive the combined cases. Therefore, methods that lower random loads would be more beneficial than the small gains from load combination schemes (see the 2σ column).

3. SPACELAB DATA

The Spacelab 1 vibration verification instrumentation consisted of high-frequency (5–2,000 Hz) and low-frequency (0–50 Hz) accelerometers. These measurements recorded the response of the Spacelab structure and represented the input to experiments and components rather than the response. The measurement locations were reviewed and a set of 10 pairs of low- and high-frequency measurements located very close to each other were selected for evaluation. Analog tapes of the measurements were obtained and digitized over a 4-sec period beginning 0.2 sec before solid rocket booster ignition. Filters were set at 40–2,000 Hz for the high-frequency measurements and 0–40 Hz for the low-frequency measurements to ensure that one measurement did not affect the other. Table 2 shows the measurements used.

Table 2. Spacelab measurement locations.

Low-Frequency Measurement	High-Frequency Measurement	Description	Axis
L05A8208	L05D8301A	Rack and floor interface	X
L05A8210	L05D8303A	Rack and floor interface	Z
L05A8207	L05D8305A	Rack and overhead attachment interface	Y
L05A8504	L05D8504A	Pallet hardpoint and component interface	X
L05A8530	L05D8506A	Pallet hardpoint and component interface	Z
L05A8512	L05D8507A	Orthogrid and component interface	X
L05A8513	L05D8508A	Orthogrid and component interface	Y
L05A8514	L05D8509A	Orthogrid and component interface	Z
L05A8108	L05D8801A	Module core	X
L05A8109	L05D8802A	Module core	Y

Once consistent sets of time history data were obtained, they were combined in various ways and statistics were calculated. Figure 3 shows a comparison of one measurement combination with a normal distribution. The data fit the normal distribution pretty well, but the cumulative distribution around the 3σ value (99.865 percent) shows about a 0.1 g difference. Figure 4 shows how the data look when combined.

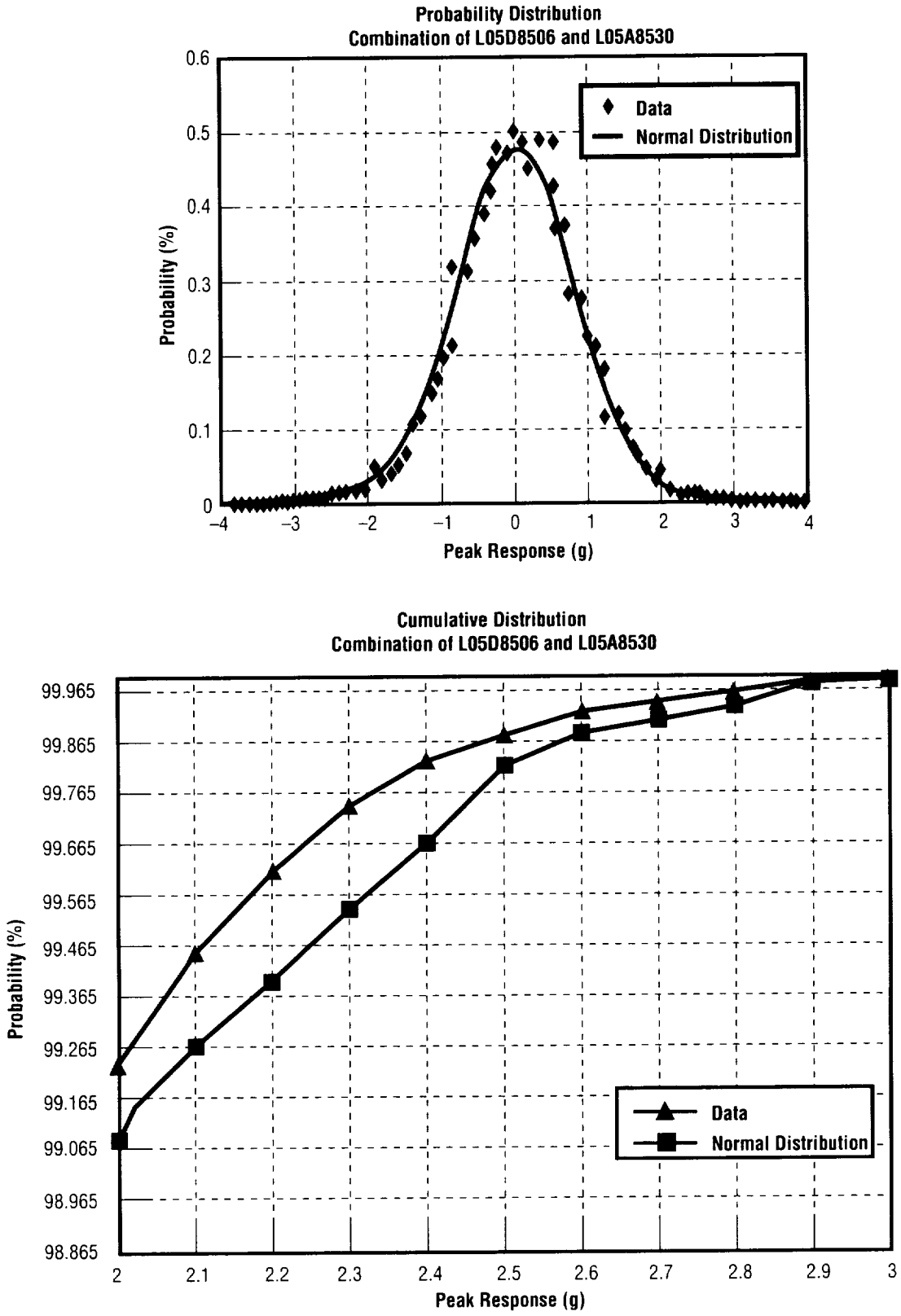

Figure 3. Comparison of Spacelab data with normal distribution.

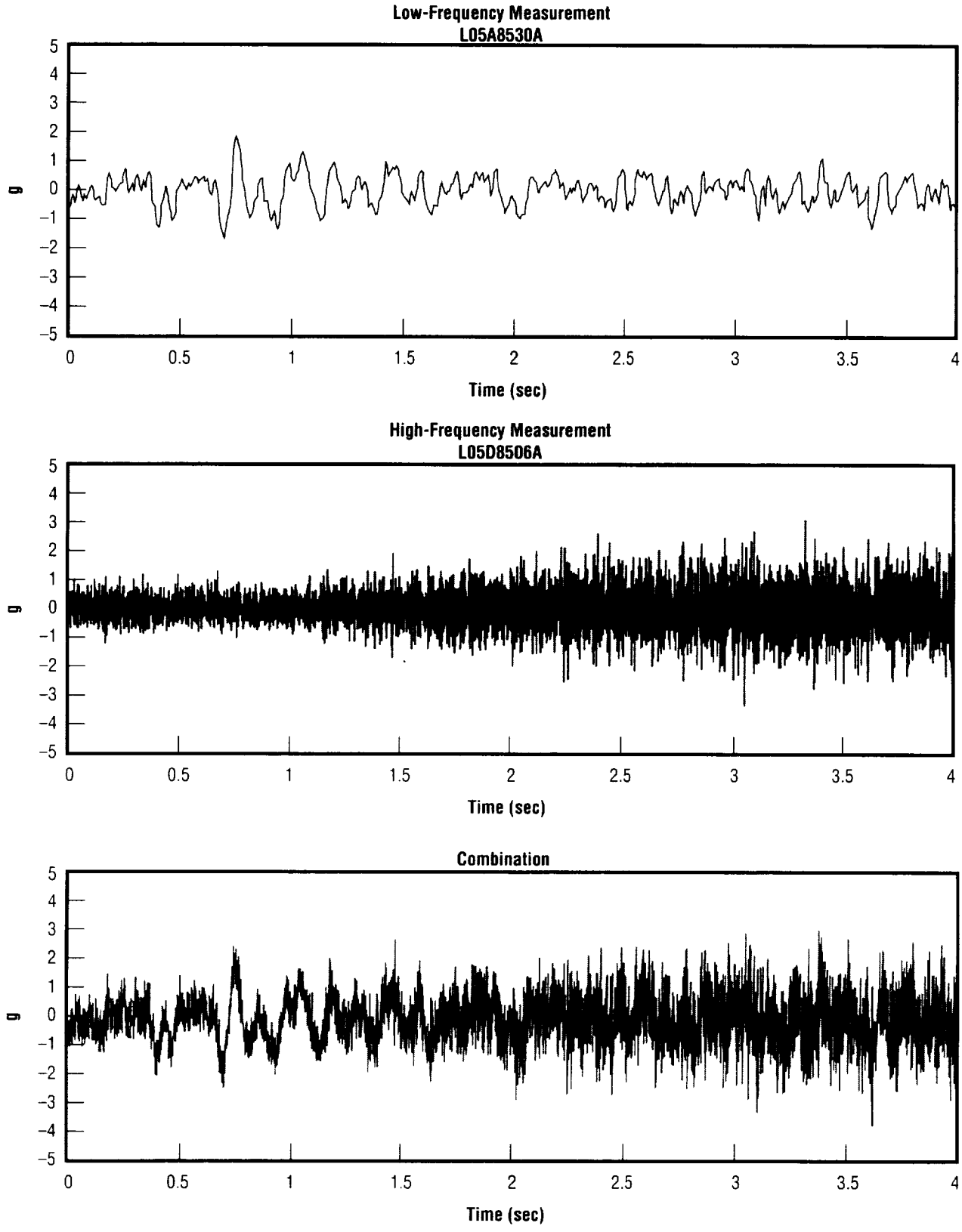

Figure 4. Typical Spacelab measurements.

The present method of combining loads is to add the predicted loads directly together, so this method (using the flight data) was used as a baseline for other methods. Table 3 shows the results of combining the entire 4-sec data blocks and picking the maximum peaks during that period. Each column is explained below. When dealing with random data it is customary to describe the amplitude statistically in terms of the standard deviation over a stationary period. After time-consistently adding the two measurements, statistics were calculated and shown in columns 7 and 8. Column 7 shows the maximum time-consistent peak during the 4-sec period while column 8 shows the level that encompasses 99.865 percent of the data. Column 8 is the 99.865-percent probability level which is the 3σ (three times

Table 3. Results of Spacelab data evaluation.

Column	Description
3	Highest peak of low-frequency measurement
4	Highest peak of high-frequency measurement
5	Maximum RMS of high-frequency measurement during 4-sec period
6	Sum of high- and low-frequency peaks regardless of timing (column 3 + column 4)
7	Maximum time-consistent peak of combined measurements
8	3σ level of combined data
9	$3\sigma + A$ (column 3 + 3 times column 5)
10	$\sqrt{A^2 + (3\sigma)^2}$
11	3σ level of combined data using Tuell and Schock method

Column 1	2	3	4	5	6	7	8	9	10	11
LF Meas.	HF Meas.	LF Peak	HF Peak	HF RMS	Sum Peaks	100%	99.9%	$3\sigma + A$	RSS	PDF
8530	8506	1.87	3.32	0.827	5.19	3.15	2.61	4.35	3.10	3.15
8504	8504	2.08	4.33	1.145	6.41	4.03	3.37	5.51	4.01	4.04
8108	8801	2.94	1.19	0.814	4.13	3.25	2.24	5.38	3.82	3.91
8109	8802	2.79	1.27	0.353	4.06	2.87	2.71	3.85	2.98	2.93
8208	8301	0.85	0.67	0.221	1.52	1.20	0.94	1.51	1.08	1.15
8210	8303	2.93	0.92	0.225	3.86	3.25	2.91	3.61	3.01	2.84
8207	8305	2.07	2.54	0.346	4.61	2.99	2.41	3.11	2.31	2.32
8512	8507	1.93	0.86	0.236	2.80	2.20	1.97	2.64	2.06	2.02
8513	8508	0.71	0.96	0.270	1.67	1.24	0.93	1.52	1.08	1.23
8514	8509	1.98	1.03	0.288	3.01	2.20	2.00	2.85	2.16	2.14

the root mean square (RMS)) level assuming that the data fit a Gaussian probability distribution. This probability level is commonly used in calculating random loads. Column 11 shows the results of applying the Tuell and Schock method[2] of combining loads. Columns 2–8 are the results of measured data while columns 9–11 are predictions based on the measured data.

The first general observation is the overall low magnitude of the numbers compared to the preflight predictions. In almost all cases the preflight predictions were significantly higher than the measured data. However, these data represent just one flight and subsequent flights could show higher responses. Presumably the highest stresses occurred during maximum acceleration (shown in column 7) and both the RSS method (column 10) and the PDF (column 11) are very close to the maximum time-consistent acceleration. Therefore, either the RSS method or the PDF would give close estimates of the maximum load if the peak low frequency and RMS high-frequency accelerations are known.

The difference between the most conservative combination method ($A + 3\sigma$) and the least (RSS) is on the order of 30–40 percent. This may seem significant but the difference between the load prediction and the measured response is much higher. This indicates that the combination may be less important than the prediction method. Unfortunately these measurements are inputs to components and the responses must be estimated using poorly defined parameters. Before the issues of load combination and prediction can be properly addressed, a flight measurement system must be designed and implemented to measure both low- and high-frequency payload responses.

4. PHASING OF HIGH-AND LOW-FREQUENCY LOADS

The relative phasing of the low- and high-frequency loads is of concern because generally the two loads are combined, assuming that the maxima of both phenomena occur simultaneously. As can be seen in figure 4, this is rarely the case. While the low-frequency transients occur at liftoff and quickly damp out, the random vibration maximum occurs soon after liftoff, usually at about T+3 to 4 sec. In an attempt to quantify the statistics of this relative phasing, the RMS time histories of the low- and high-frequency measurements on Spacelab 1 were calculated and plotted together, as shown in figure 5 and appendix A (figs. 6–14). Each measurement was normalized to its maximum value, so the magnitudes on the plots are only relative to the individual measurements. The rest of the measurements are shown in appendix B (figs. 15–23).

No general assumptions about phasing can be made from the limited data sample from Spacelab 1. For example, the module core Z measurements show that at T+3.5 sec, 75 percent of the transient is still present when the high-frequency measurement approaches its maximum value. Johnson Space Center has proposed that design loads should be calculated by adding 50 percent of the random load to 100 percent of the transient load. This would underestimate the design load for the module Z case and all loads where the high-frequency load is much higher than the transient. A better method would take the highest of (X%)A + 100%R and 100%A + (X%)R, where A and R are the transient and random loads, respectively. X must be agreed upon by all parties and based upon concrete data.

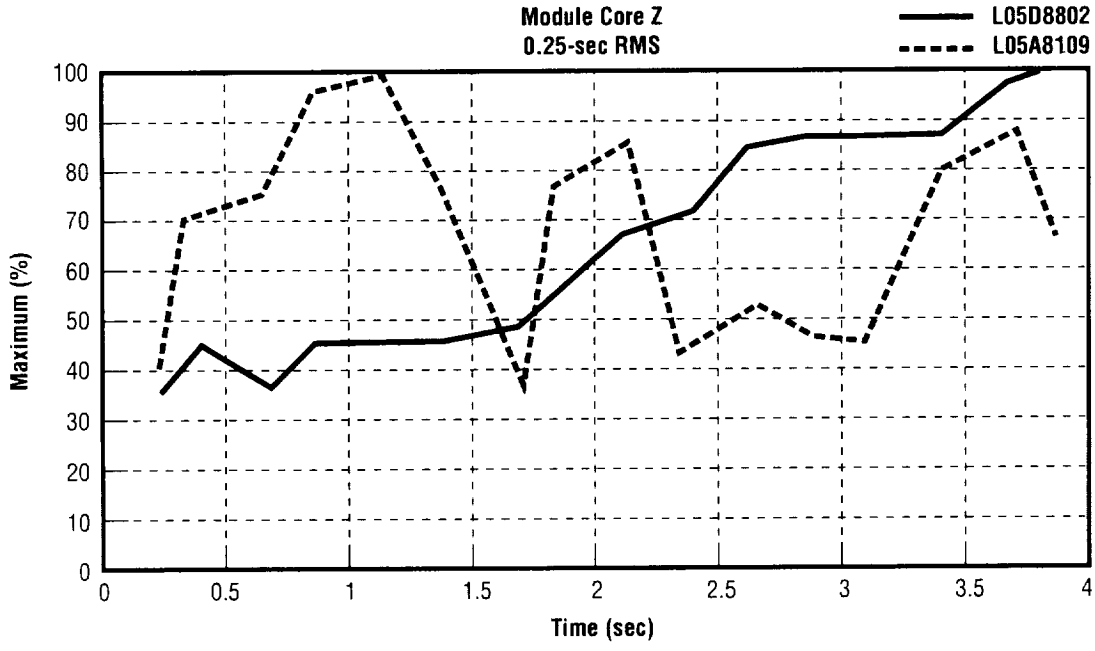

Figure 5. Occurence of maximum levels of low- and high-frequency measurements.

5. CONCLUSIONS

The results of this study point out the need for additional research into load prediction technology and correlation with actual flight results. The conclusions drawn from sections 2 and 3 are:

- The best combination method is RSS, which closely approximates the Tuell and Schock (most exact) method.
- Random load prediction technology has a great influence on the final limit load calculation.
- The relative phasing of the maximum low- and high-frequency loads is inconsistent and no general conclusions can be drawn from the limited flight data.

The limited flight data examined points out the need for specialized instrumentation on future flights to better correlate actual loads experienced by payload components during flight with the pre-flight predictions. In particular, random load technology can be improved and large reductions in limit loads achieved by time-consistently combining transient and random loads. Future research programs can concentrate on these areas.

APPENDIX A—Time History Plots of Spacelab Measurements

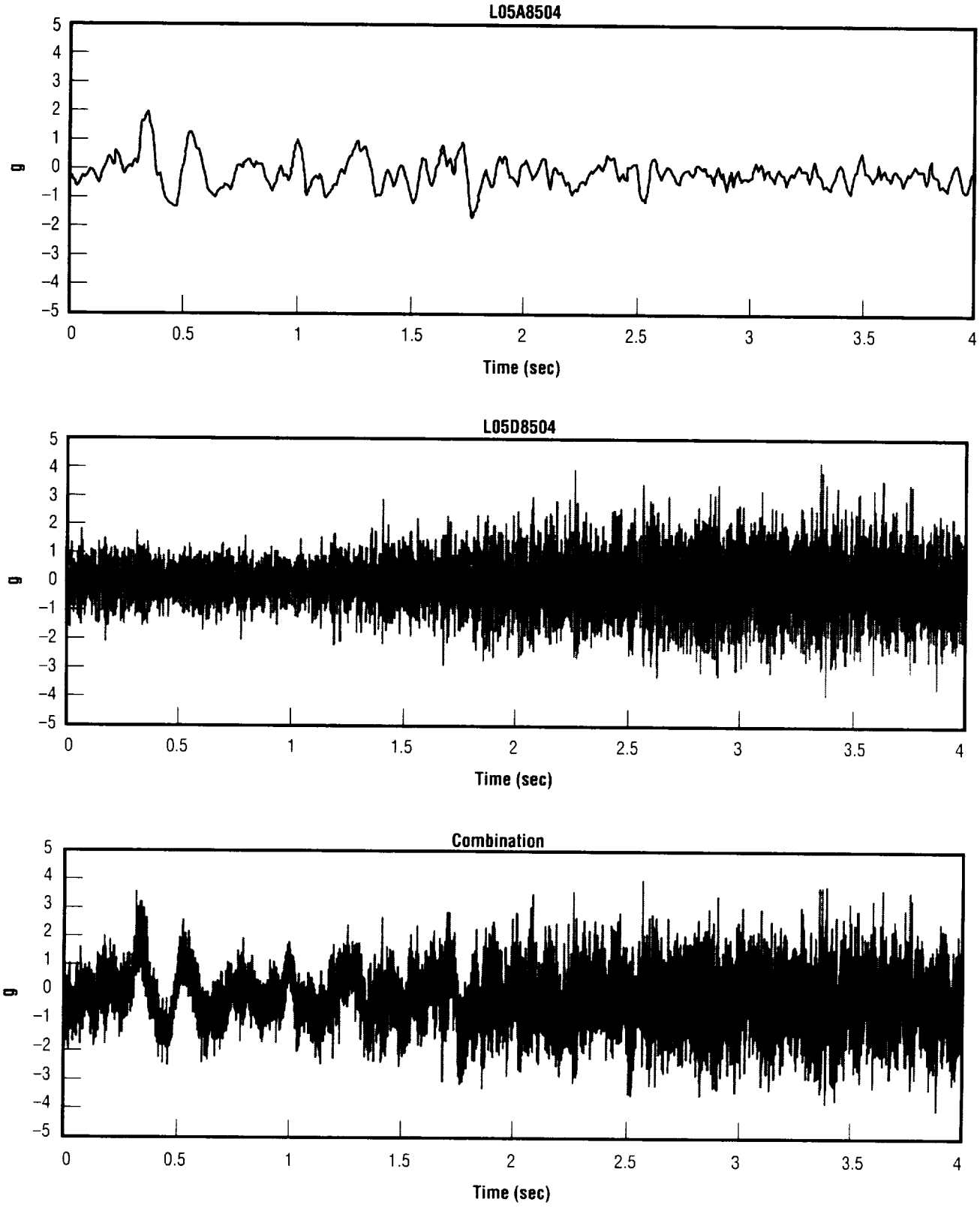

Figure 6. Pallet hardpoint and component interface.

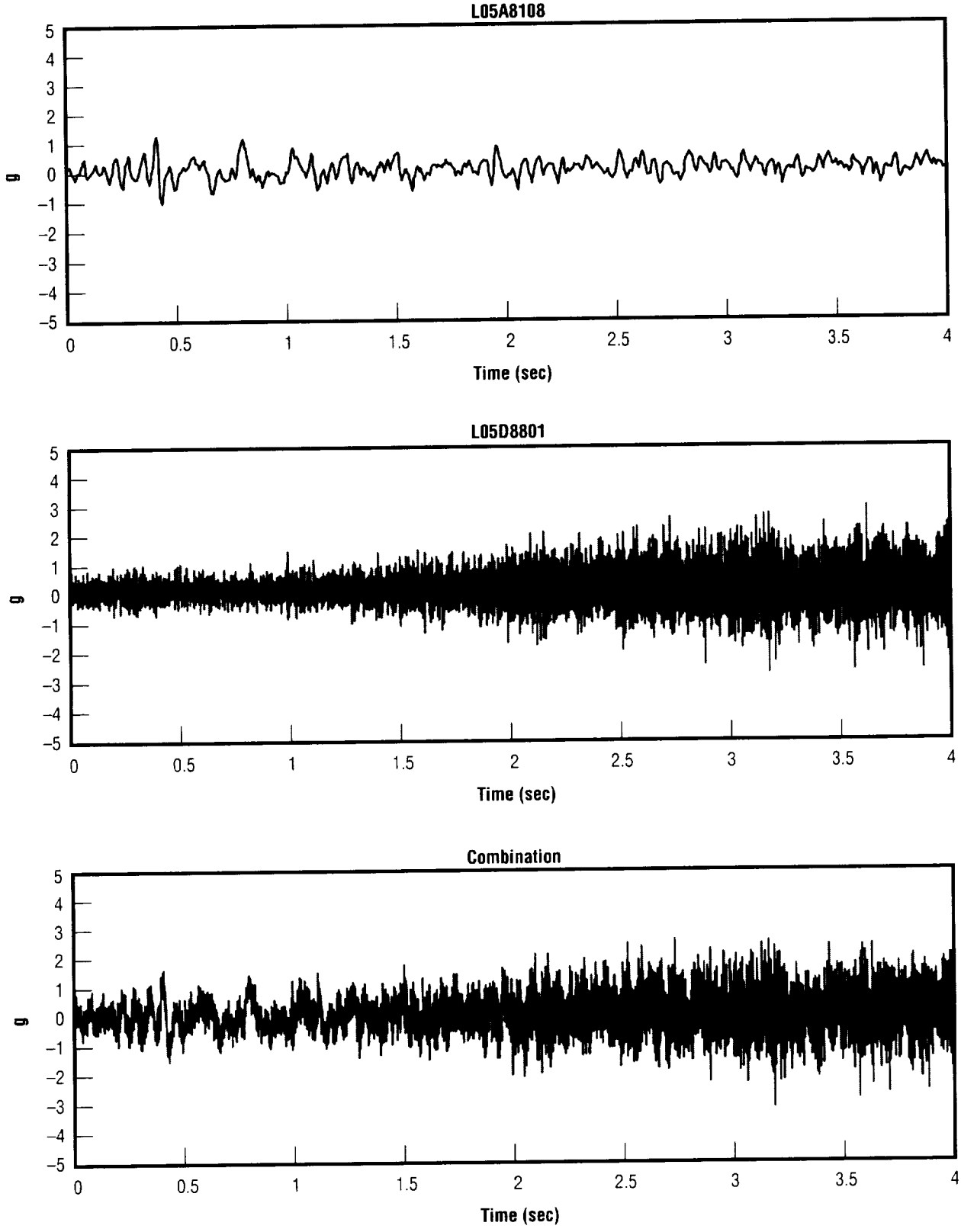

Figure 7. Module core X.

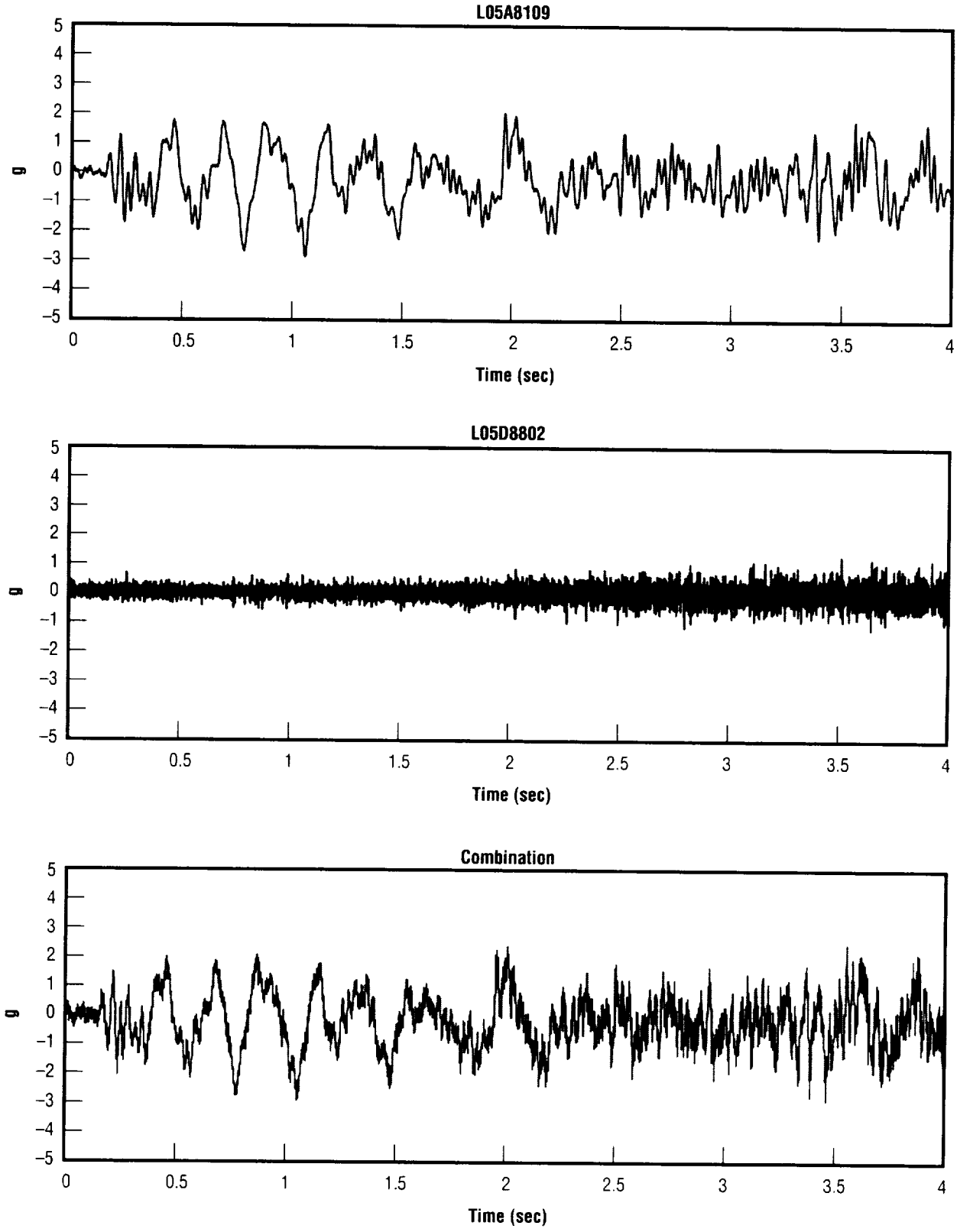

Figure 8. Module core Y.

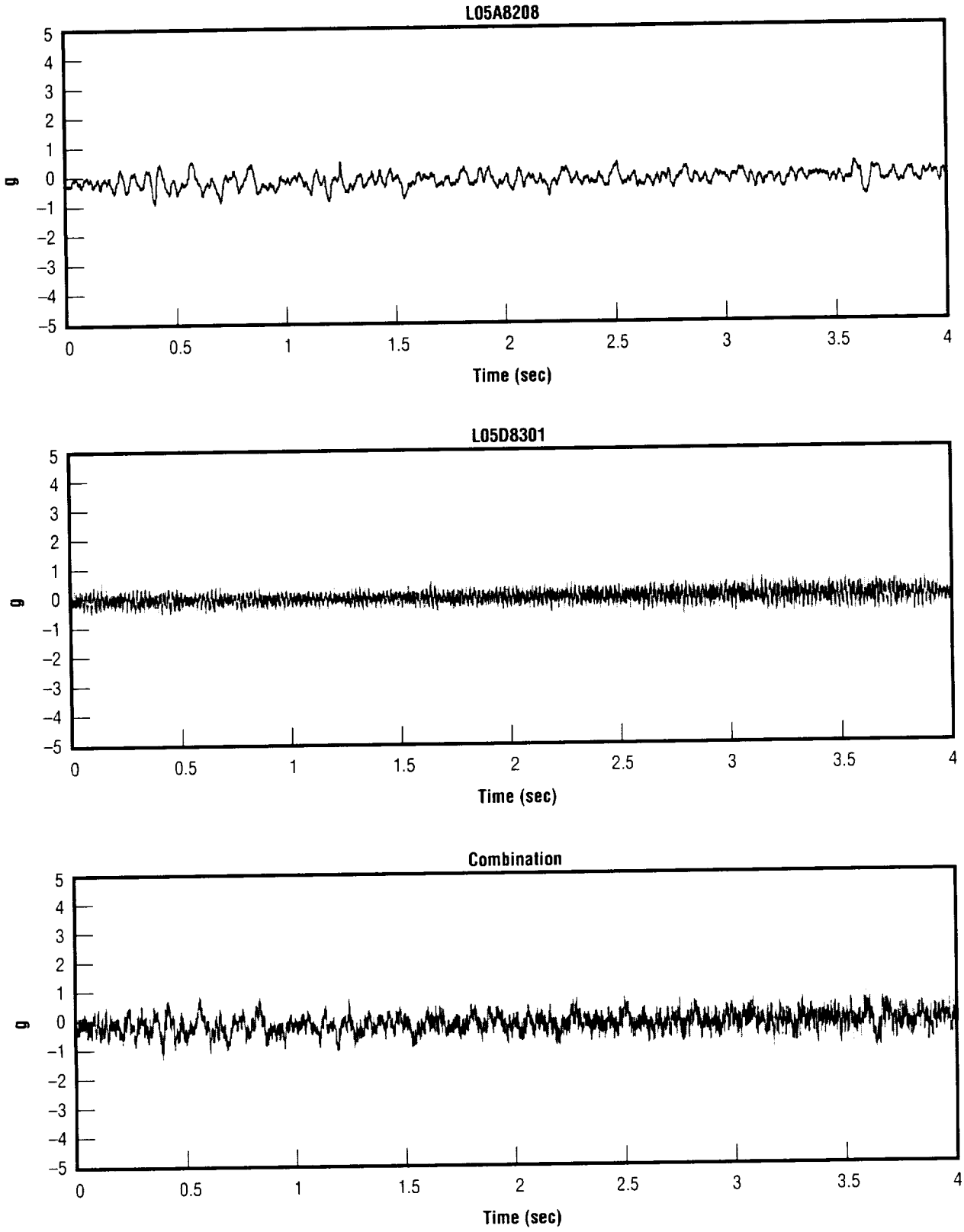

Figure 9. Rack and floor interface X.

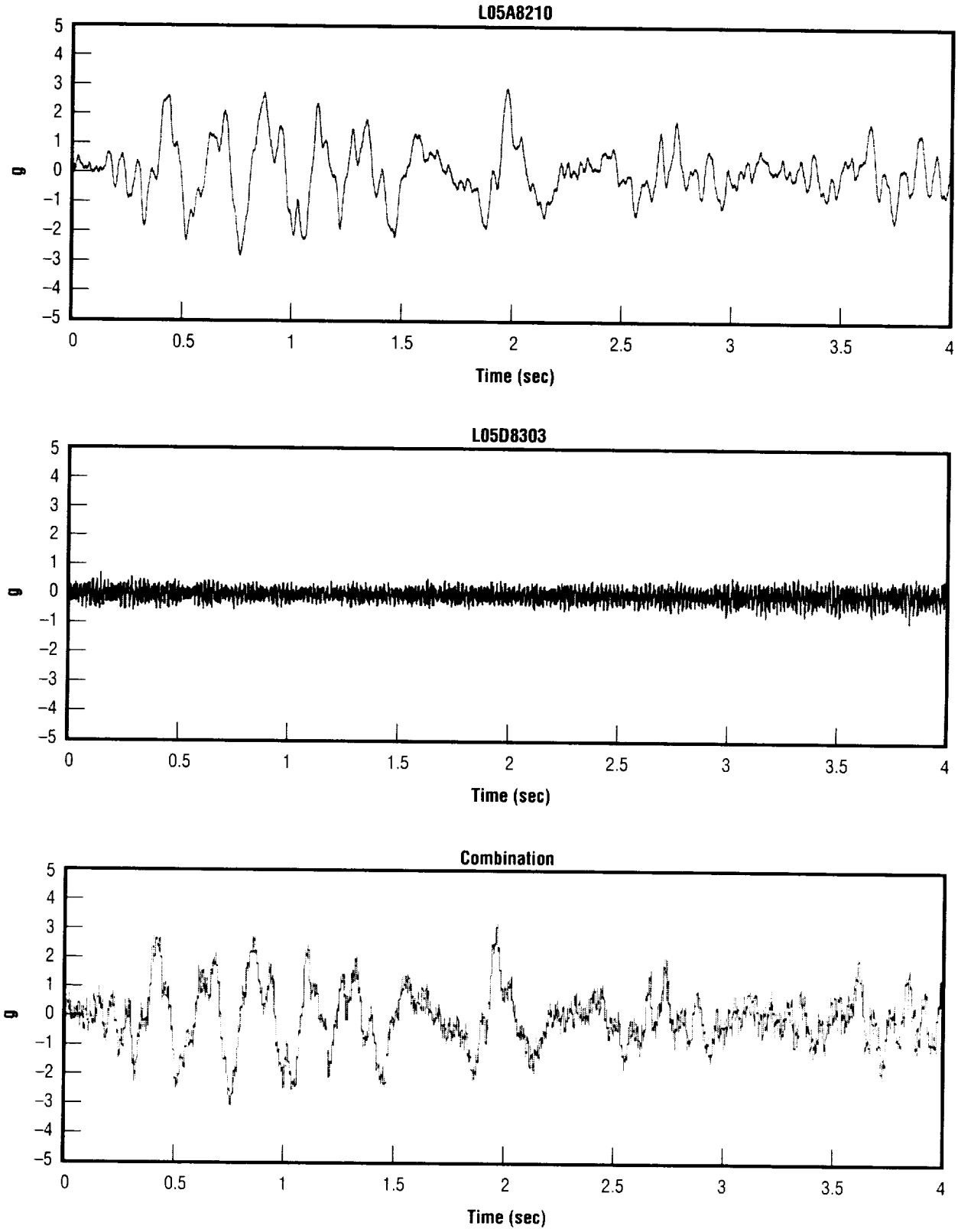

Figure 10. Rack and floor interface Z.

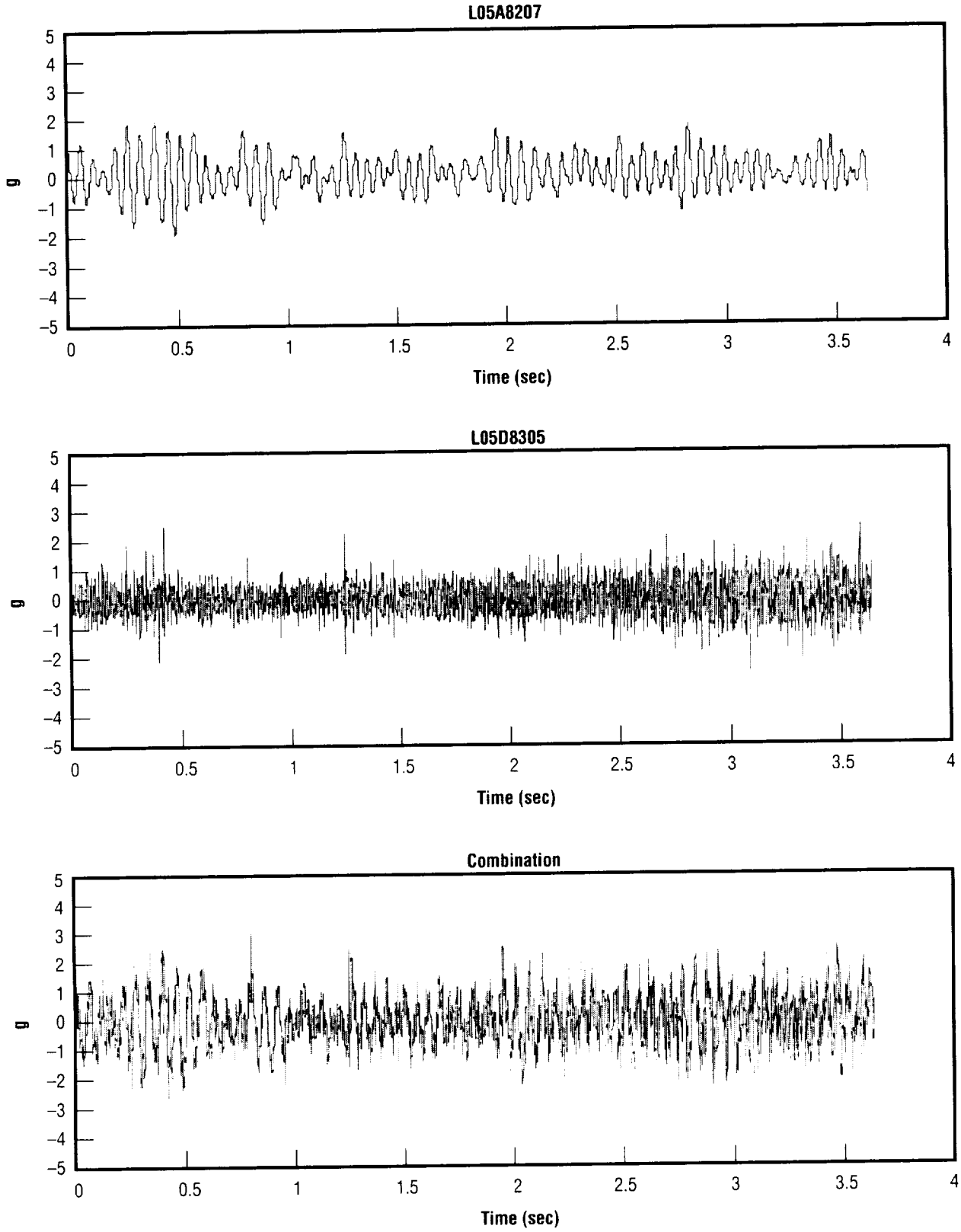

Figure 11. Rack and overhead attachment interface.

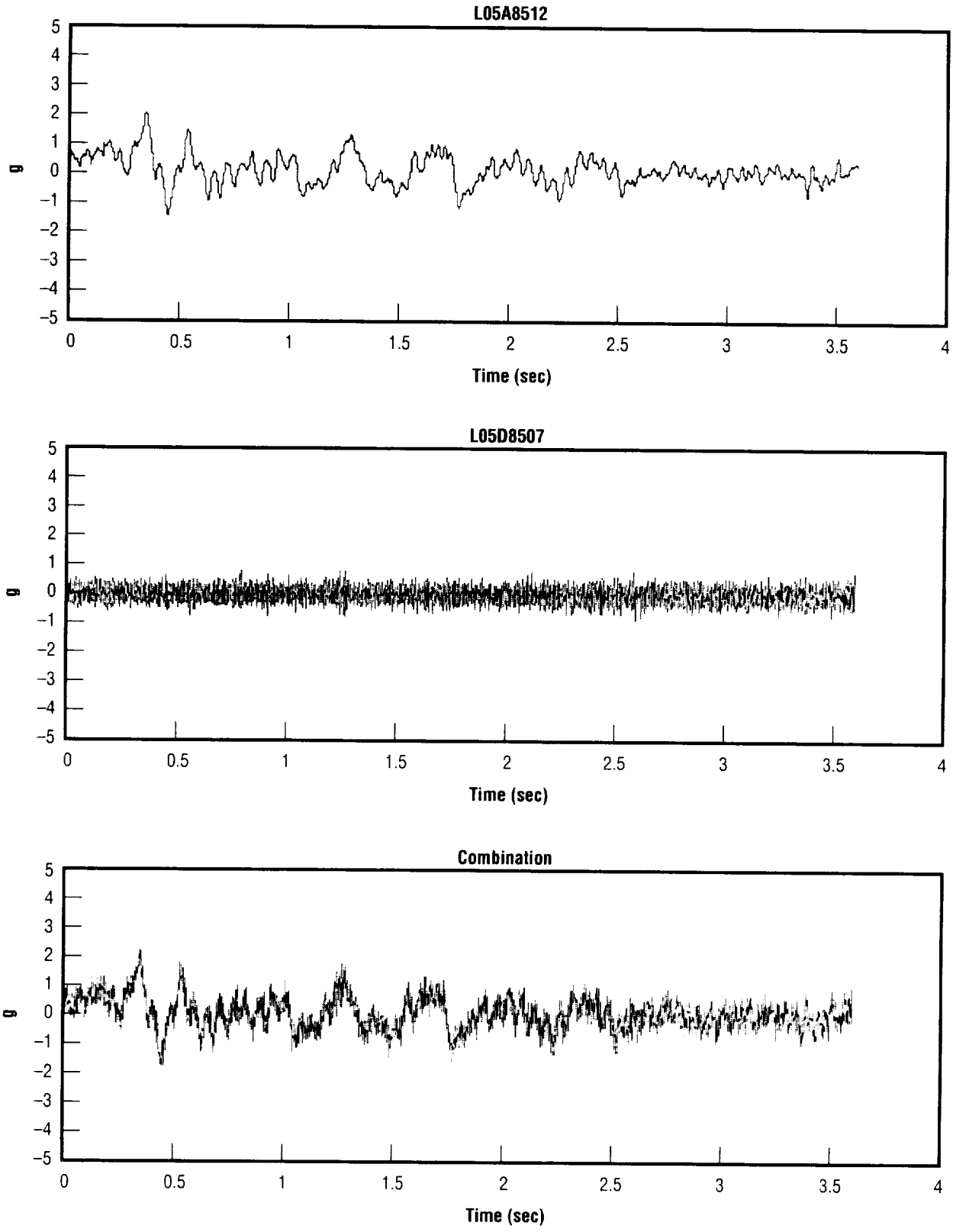

Figure 12. Orthogrid and component interface X.

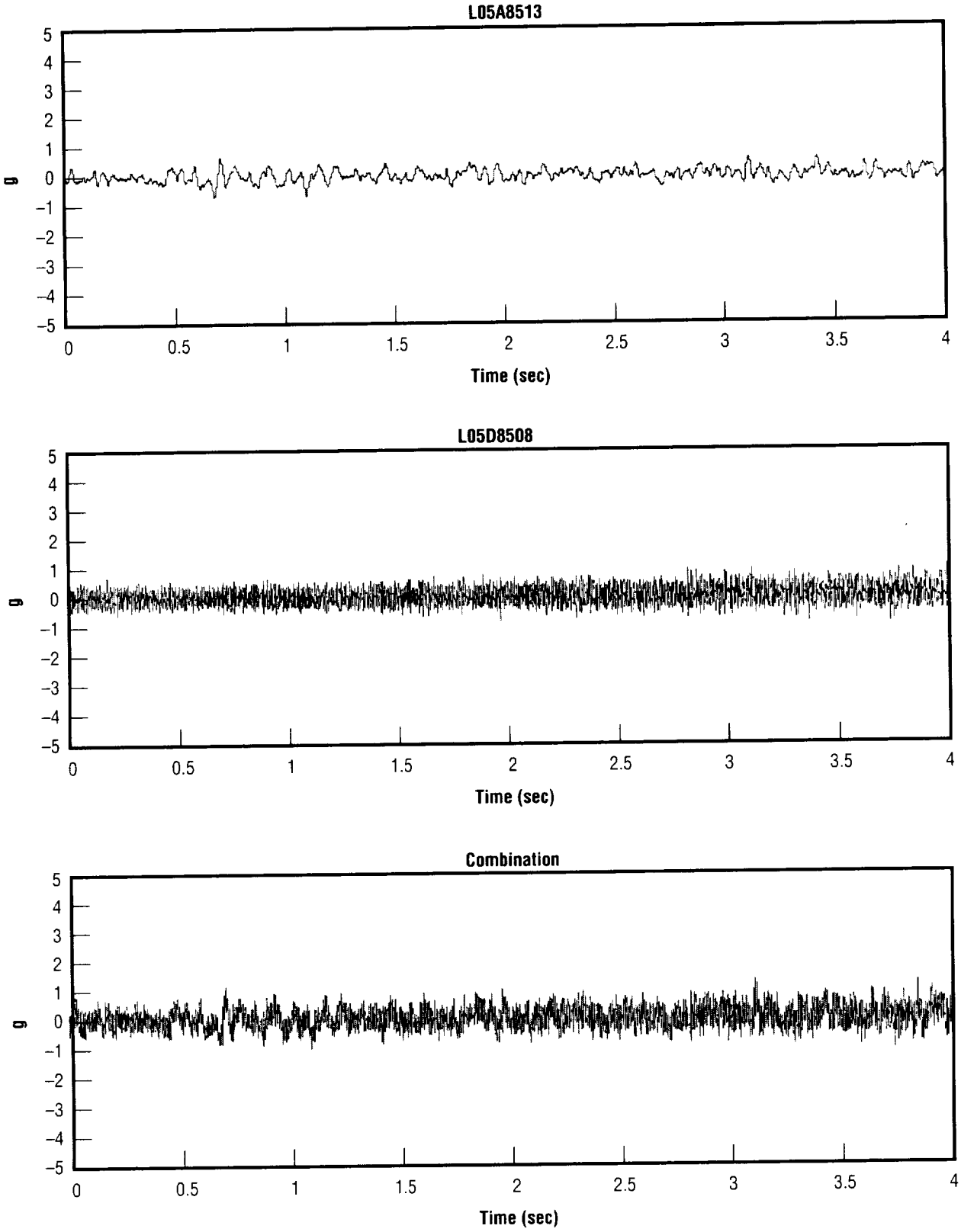

Figure 13. Orthogrid and component interface Y.

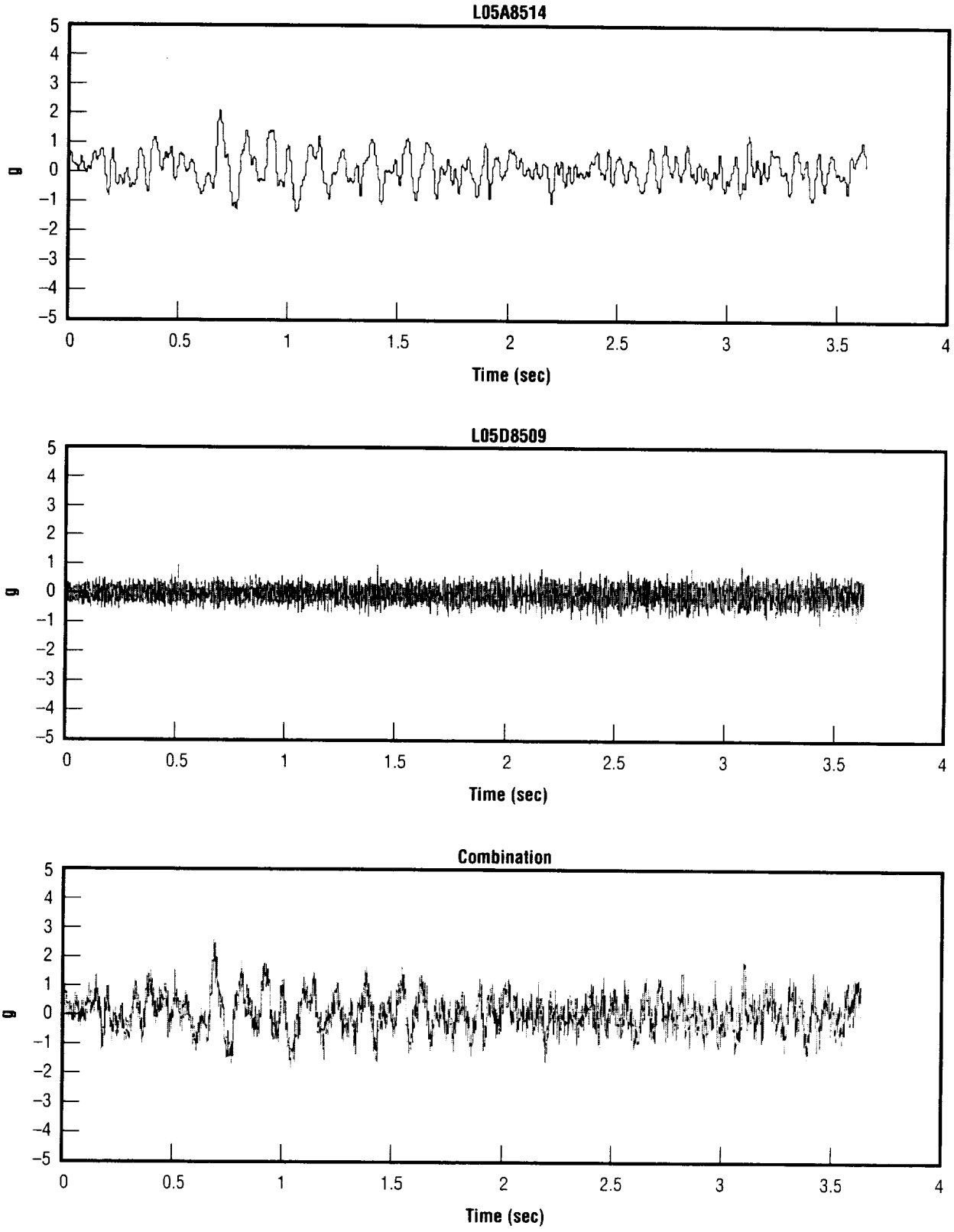

Figure 14. Orthogrid and component interface Z.

APPENDIX B—Occurrence of Maximum Levels in Spacelab Data

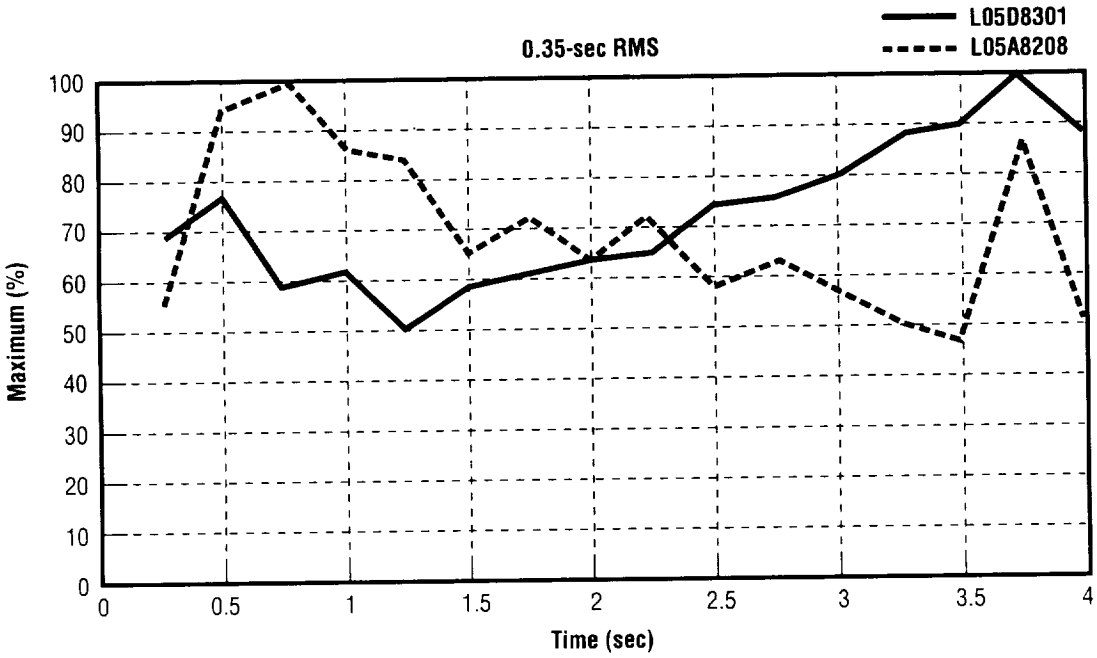

Figure 15. Rack 4 bottom X direction.

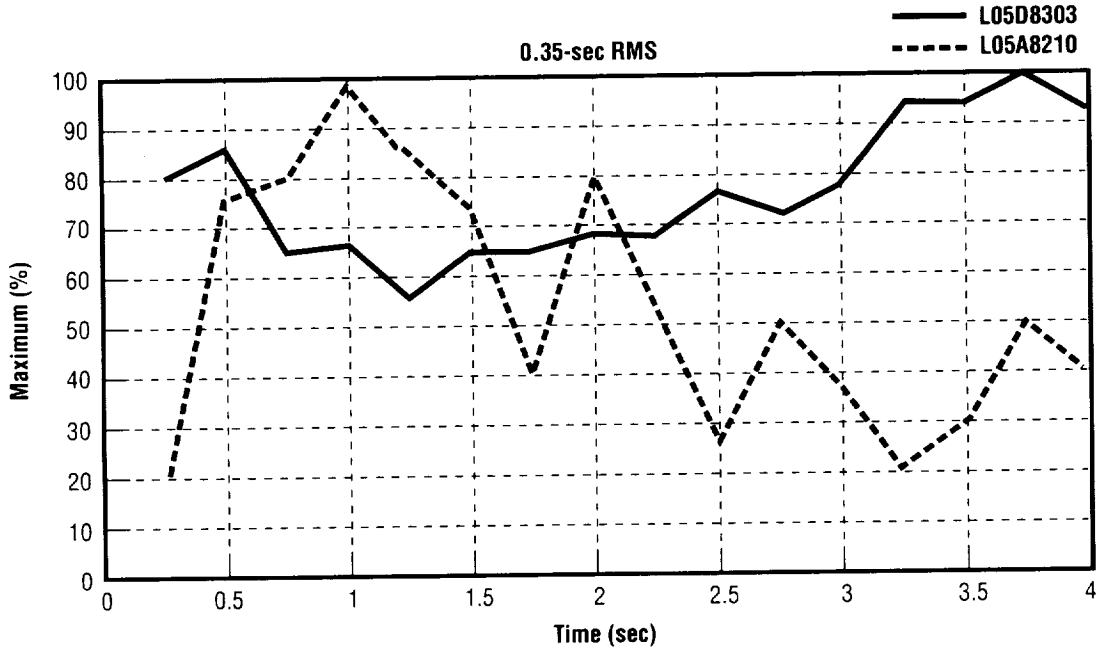

Figure 16. Rack 4 bottom Z direction.

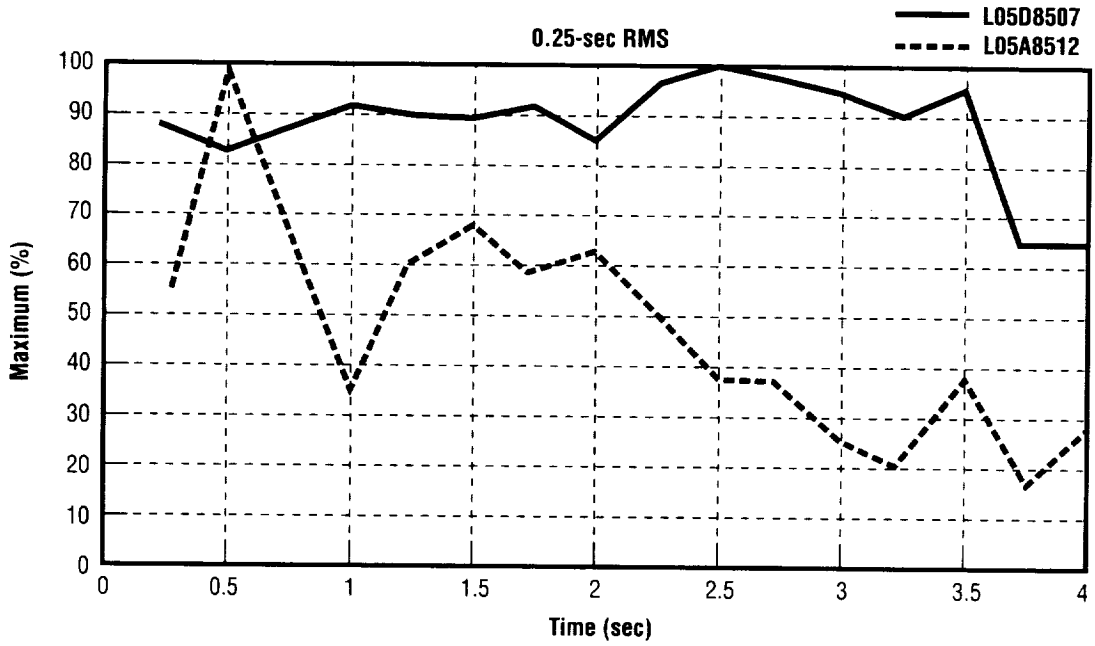

Figure 17. Orthogrid top X direction.

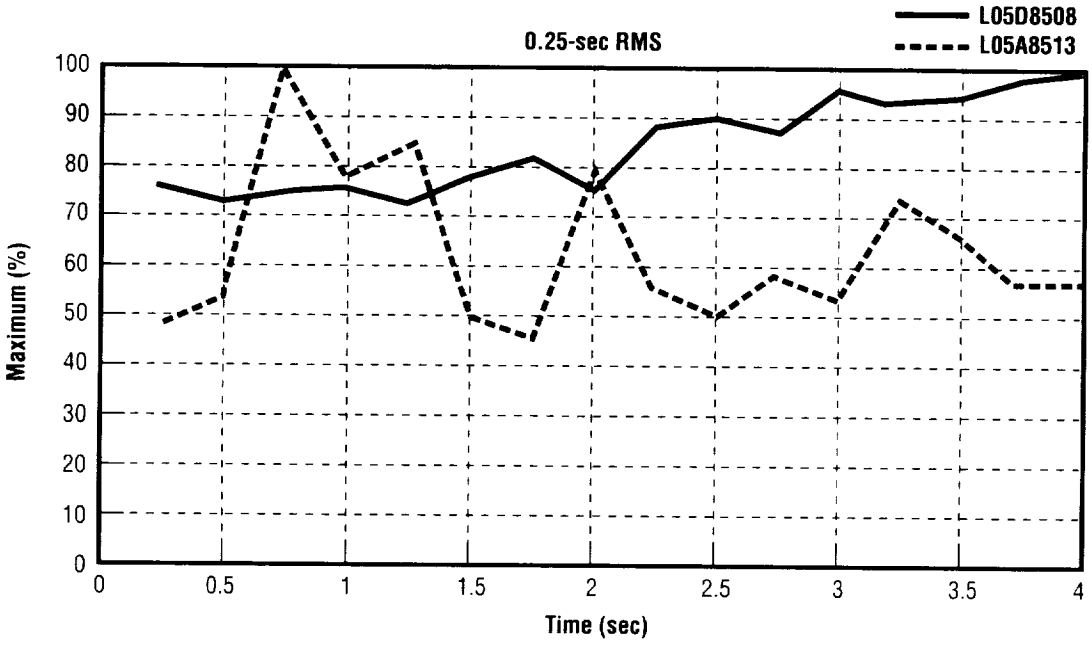

Figure 18. Orthogrid top Y direction.

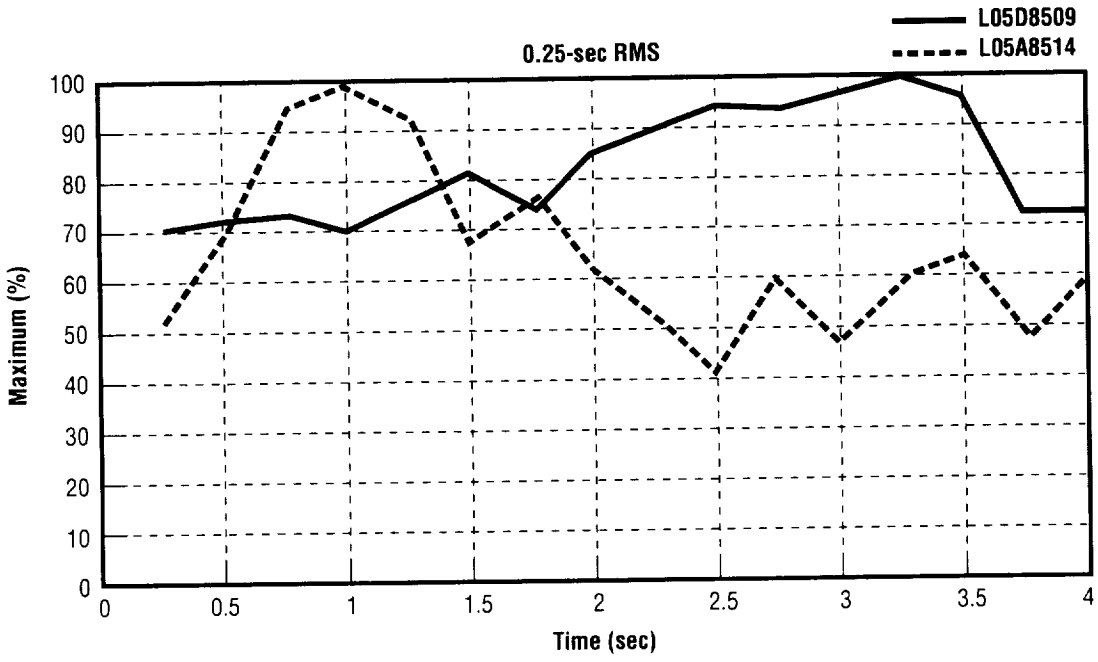

Figure 19. Orthogrid top Z direction.

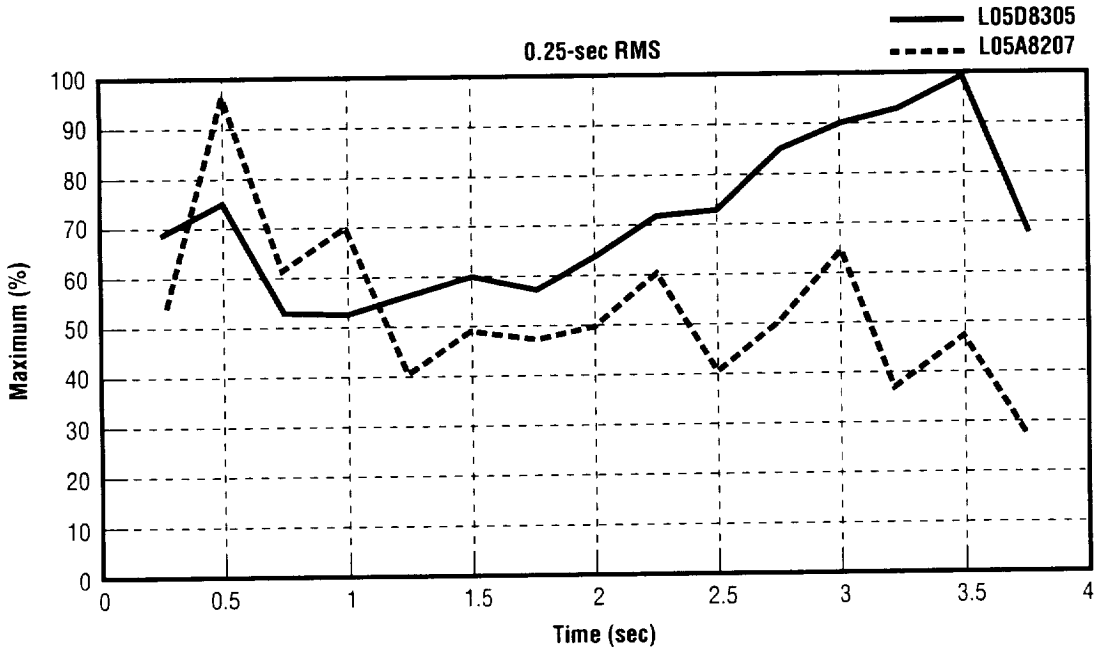

Figure 20. Rack top Y.

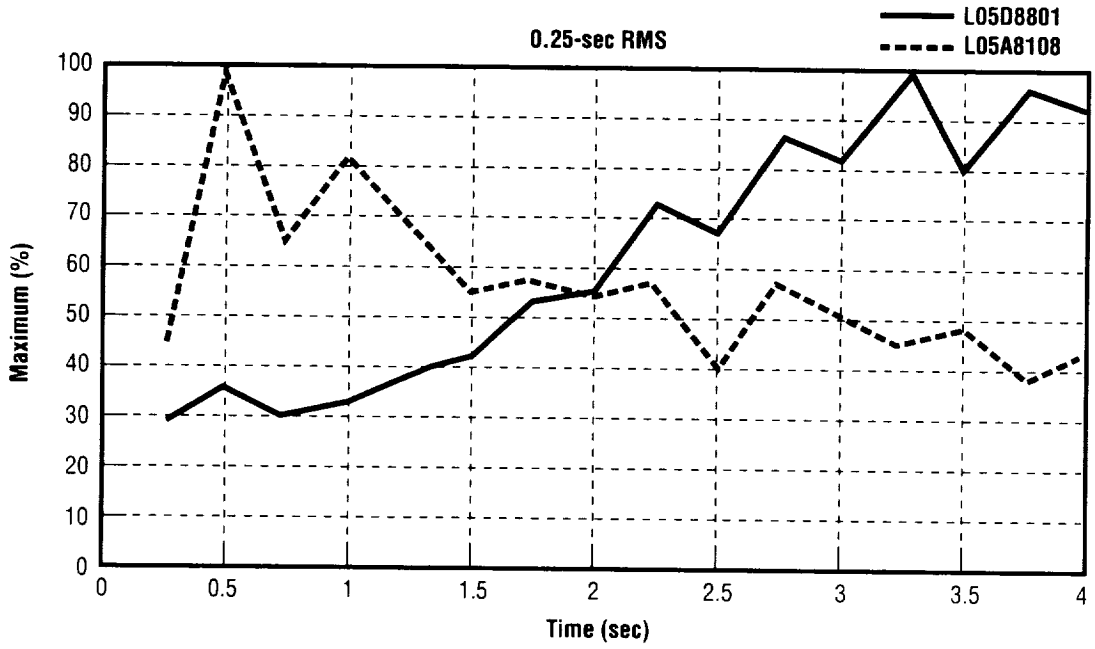

Figure 21. Module core Y.

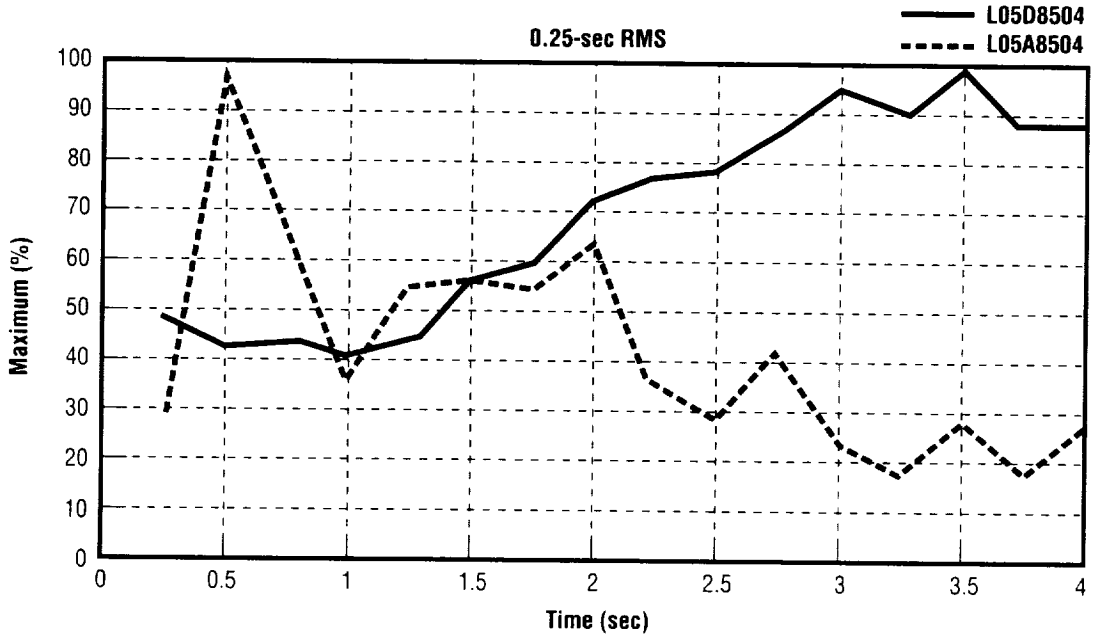

Figure 22. Pallet X.

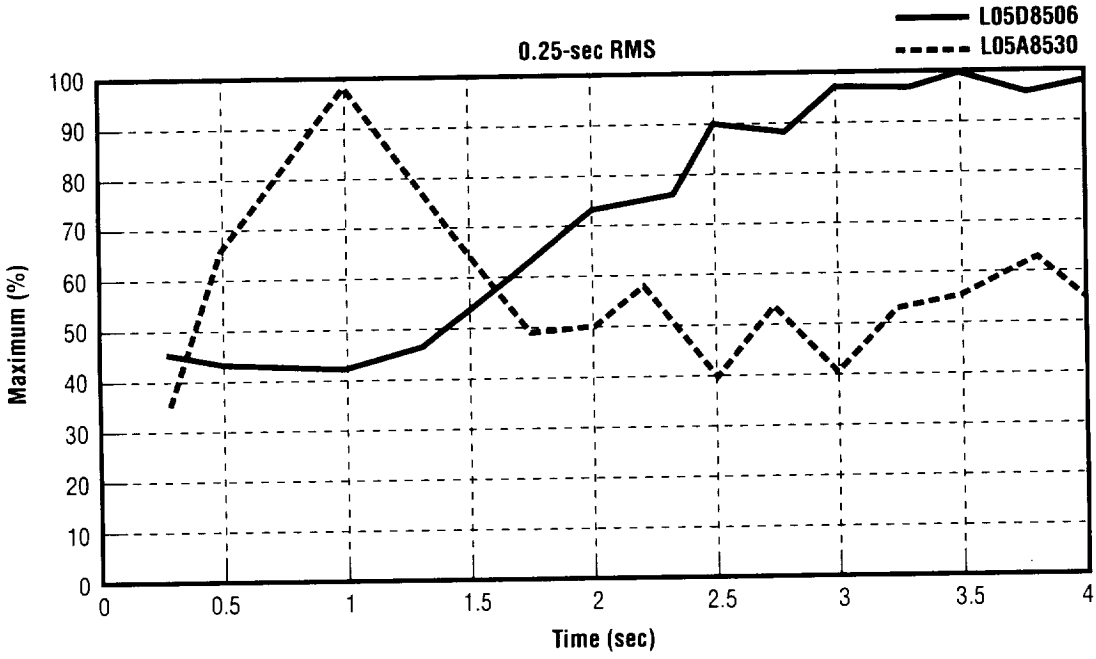

Figure 23. Pallet Z.

REFERENCES

1. Ferebee, R.C.; and Jones, J.H.: "Comparison of Miles' Relationship to the True Mean Square Value of Response for a Single Degree of Freedom System," Shuttle Dynamic Environment and Loads Prediction Workshop, Pasadena, CA, January 1984.

2. Schock, R.W.; and Tuell, L.P.: "An Investigation into the Probabilistic Combination of Quasi-Static and Random Accelerations," *NASA-TM-82584*, May 1, 1984.

REPORT DOCUMENTATION PAGE

Form Approved
OMB No. 0704-0188

1. AGENCY USE ONLY *(Leave Blank)*	2. REPORT DATE	3. REPORT TYPE AND DATES COVERED
	June 2000	Technical Memorandum

4. TITLE AND SUBTITLE
Loads Combination Research at Marshall Space Flight Center

5. FUNDING NUMBERS

6. AUTHORS
R. Ferebee

7. PERFORMING ORGANIZATION NAMES(S) AND ADDRESS(ES)
George C. Marshall Space Flight Center
Marshall Space Flight Center, Alabama 35812

8. PERFORMING ORGANIZATION REPORT NUMBER
M–981

9. SPONSORING/MONITORING AGENCY NAME(S) AND ADDRESS(ES)
National Aeronautics and Space Administration
Washington, DC 20546–0001

10. SPONSORING/MONITORING AGENCY REPORT NUMBER
NASA/TM— 2000–210331

11. SUPPLEMENTARY NOTES
Prepared by Structures, Mechanics, and Thermal Department, Engineering Directorate

12a. DISTRIBUTION/AVAILABILITY STATEMENT
Unclassified-Unlimited
Subject Category 18
Nonstandard Distribution

12b. DISTRIBUTION CODE

13. ABSTRACT *(Maximum 200 words)*

This is the result of a study conducted by the Structural Dynamics Division of the Marshall Space Flight Center concerning the combination of low- and high-frequency dynamic loads for spacecraft design. Low-frequency transient loads are combined with high frequency acoustically induced loads to arrive at a limit load, for design purposes. Different methods are used for combining the loads which can lead to considerable variation in limit loads, depending on which NASA Center did the calculation. This study investigates several different combination methods and compares the combination methods with Spacelab 1 flight data. In addition, the relative timing of low- and high-frequency loads is examined.

14. SUBJECT TERMS	15. NUMBER OF PAGES
transient loads, random loads, load combination, acoustically induced loads, Miles' Relationship	36
	16. PRICE CODE A03

17. SECURITY CLASSIFICATION OF REPORT	18. SECURITY CLASSIFICATION OF THIS PAGE	19. SECURITY CLASSIFICATION OF ABSTRACT	20. LIMITATION OF ABSTRACT
Unclassified	Unclassified	Unclassified	Unlimited

National Aeronautics and
Space Administration
AD33
George C. Marshall Space Flight Center
Marshall Space Flight Center, Alabama
35812